

# A prototype MRPC beam test for the BESIII ETOF upgrade<sup>\*</sup>

SUN Yong-Jie(孙勇杰)<sup>1</sup> YANG Shuai(杨帅)<sup>1</sup> LI Cheng(李澄)<sup>1;1)</sup> QIAN Sen(钱森)<sup>2</sup>  
XU Lai-Lin(徐来林)<sup>1</sup> FU Zai-Wei(付在伟)<sup>2</sup> HENG Yue-Kun(衡月昆)<sup>2</sup>  
CHEN Hong-Fang(陈宏芳)<sup>1</sup> TANG Ze-Bo(唐泽波)<sup>1</sup>  
SHAO Ming(邵明)<sup>1</sup> LIU Huan-Huan(刘欢欢)<sup>1</sup>

<sup>1</sup> Department of Modern Physics, University of Science and Technology of China, Hefei 230026, China

<sup>2</sup> Institute of High Energy Physics, Chinese Academy of Sciences, Beijing 100049, China

**Abstract:** A prototype multi-gap resistive plate chamber (MRPC) with a  $2\times 6$  gap structure is developed for the upgrading of the endcap time-of-flight (ETOF) detector in the Beijing Spectrometer (BESIII). The prototype MRPC is tested in the E3 beam line of the Beijing Electron Positron Collider (BEPC) with secondary charged particles ( $\pi$  and  $p$ , etc) of 600 MeV/c. The test results show that the time resolution of the MRPC can reach 50 ps and that the detection efficiency is greater than 98%.

**Key words:** BESIII, ETOF, MRPC, beam test

**PACS:** 29.40.Cs      **DOI:** 10.1088/1674-1137/36/5/008

## 1 Introduction

The time-of-flight (TOF) detector, devised through high time resolution detectors, is critical in particle identification for both nuclear and particle physics experiments. Fast scintillator readout by fast photomultiplier tubes (PMT) are fundamental in TOF detector building and have been widely used in many experiments, such as the current BESIII TOF, which combine scintillators and fine-mesh PMTs. With the current time resolution of 110 ps for muons, 138 ps for  $\pi$  and 148 ps for electrons, the average  $K/\pi$  separation ( $2\sigma$ ) is around 1.1 GeV [1]. If the time resolution of ETOF could be enhanced to  $\sim 50$  ps, the corresponding  $K/\pi$  separation ( $2\sigma$ ) would be extended to greater than 1.4 GeV. Thus, the particle identification (PID) capability of BESIII will be significantly improved.

In recent years, the multi-gap resistive plate chamber (MRPC), as a newly developed gaseous detector, has become one of the best choices for TOF detectors [2–5]. It has a variety of advantages such

as good time resolution, high detection efficiency, low cost and simple structure [6, 7]. In the case of BESIII, the structural characteristics of MRPC can reduce the secondary effects caused by the material before ETOF since it has smaller readout units. A proposal was raised to upgrade the current BESIII ETOF with MRPC, aiming at an intrinsic time resolution of less than 50 ps. For this purpose, an MRPC prototype with pad readout was constructed, and a beam test was performed at the BEPC E3 line using secondary particles.

## 2 The MRPC structure

The prototype MRPC is configured into a trapezium shape as shown in Fig. 1 to fully cover the BESIII endcap. This MRPC module has  $2\times 12$  readout pads 2.5 cm wide, while the length ranges from 4.0 cm to 7.0 cm. Floating glass sheets are used as the resistive plates. The thicknesses are 0.4 mm and 0.55 mm for the inner and outer glass, respectively, and the spaces between the glass layers, are  $2\times 6$  gas gaps made by a

---

Received 26 August 2011, Revised 2 December 2011

<sup>\*</sup> Supported by National Natural Science Foundation of China (10979003, 10875120) and Major State Basic Research Development Program (2008CB817702)

1) E-mail: licheng@ustc.edu.cn

©2012 Chinese Physical Society and the Institute of High Energy Physics of the Chinese Academy of Sciences and the Institute of Modern Physics of the Chinese Academy of Sciences and IOP Publishing Ltd

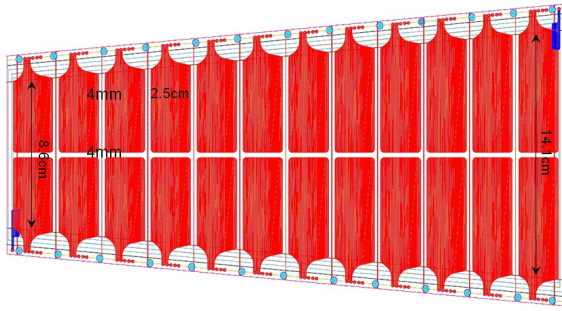


Fig. 1. The top view of the MRPC schematic.

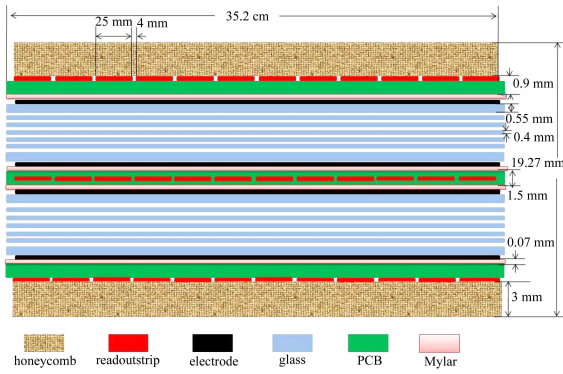


Fig. 2. The side view of the MRPC schematic.

fishing line 0.22 mm in diameter. The electrodes are made of carbon tape with a surface resistivity of  $\sim 200 \text{ k}\Omega/\square$ , attached on the surface of the outer glass and connected to the high voltage (HV) supplier. Two honeycomb boards 3 mm thick are fixed to the surface of the detector to avoid structural deformation (Fig. 2). The MRPC is placed in a gas-tight aluminum box, which is supplied with a standard atmosphere gas mixture. The component of the gas is 90% Freon + 5%  $\text{SF}_6$  + 5% iso- $\text{C}_4\text{H}_{10}$  for the test.

### 3 The beam test system

Figure 3 shows a schematic setup of the beam test system at the BEPC E3 line. Firstly, the electron beam accelerated by the linear accelerator hits

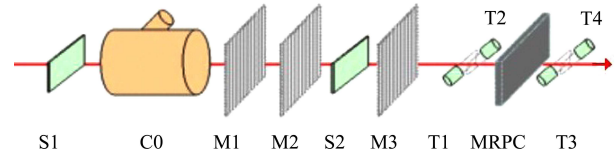


Fig. 3. The schematic setup of the beam test system.

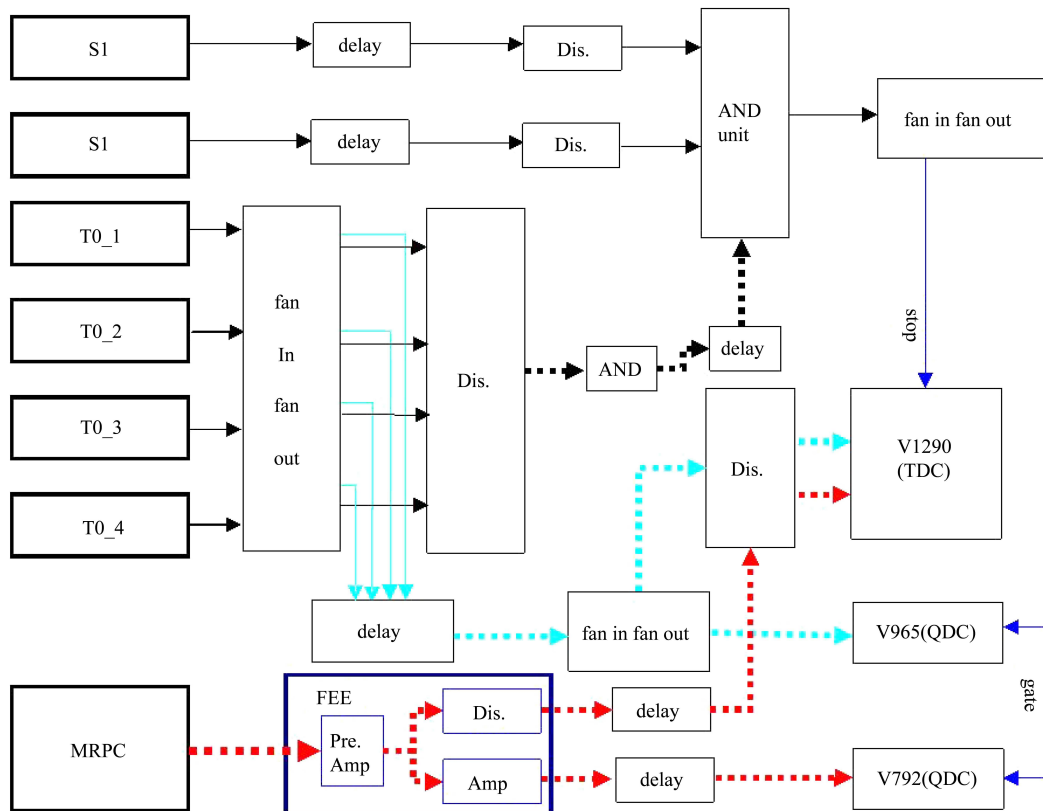


Fig. 4. The logic diagram of the DAQ.

the carbon target, producing secondary charged particles ( $e^\pm$ ,  $\pi^\pm$ , p, etc) [8]. The momentum of the charged particles used in this beam test experiment is 600 MeV/c. Two plastic scintillator detectors (S1 and S2) are used to distinguish  $\pi$  from p or e from p, while the Cerenkov detector (C0) is used to distinguish e from the hadron. Moreover, multi-wire proportional chambers (MWPC, M1, M2 and M3) are used to track the charged particles, providing the position information of the incident particles. The MWPC data were acquired by a separate CAMAC system and were not used in this test. Four 7 cm $\times$ 2 cm $\times$ 0.5 cm scintillators (T1, T2, T3 and T4) provide the reference time ( $T_0$ ). The MRPC, the detector under test, is located between T1, T2 and T3, T4. Fig. 4 is a logic diagram of the data acquisition system (DAQ). The common trigger comes from the coincidence of the signals of S1, S2 and the  $T_0$  system acting as the gate signal for the QDC and the stop signal for the TDC. The signals from both the  $T_0$  system and the MRPC, after leading edge discrimination, are sent to the TDC (VME V1290) for timing measurement. These signals are also sent to the QDC (VME V792 for MRPC and VME V965 for  $T_0$ , respectively) for charge measurement after proper delay.

#### 4 Data analysis and test results

In order to measure the time resolution of MRPC, the jitter of  $T_0$  should be determined first. Fig. 5 schematically shows the setup of the  $T_0$  system. The time recorded by the VME TDC V1290 (namely  $T_1$ ,  $T_2$ ,  $T_3$ ,  $T_4$  and  $T_{\text{MRPC}}$  for the four PMTs and MRPC, respectively) is relative to the same clock reference.

The reference time  $T_0 = (T_1 + T_2 + T_3 + T_4)/4$  has the same deviation as  $(T_1 + T_2 - T_3 - T_4)/4$ , while the latter does not include the clock reference. So we use  $(T_1 + T_2 - T_3 - T_4)/4$  to calculate the jitter of  $T_0$ .

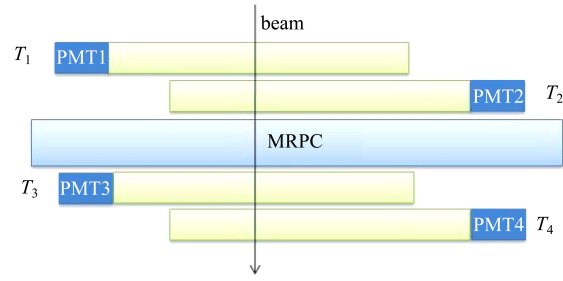


Fig. 5. The schematic of the  $T_0$  system.

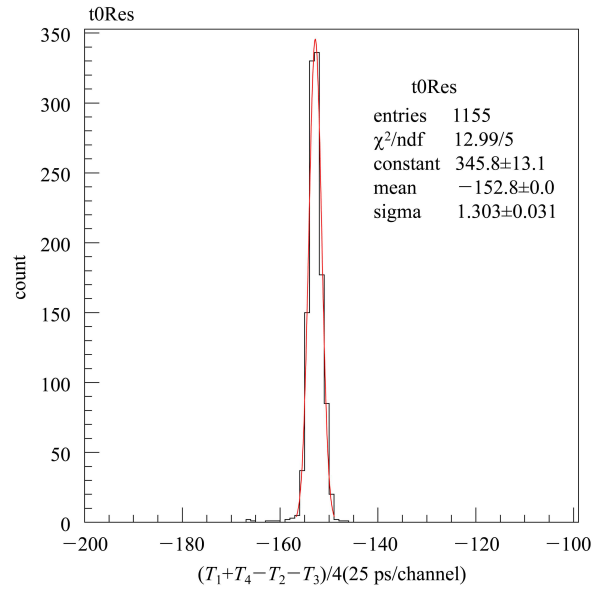


Fig. 6. The time spectrum of  $T_0$  after T-A correction.

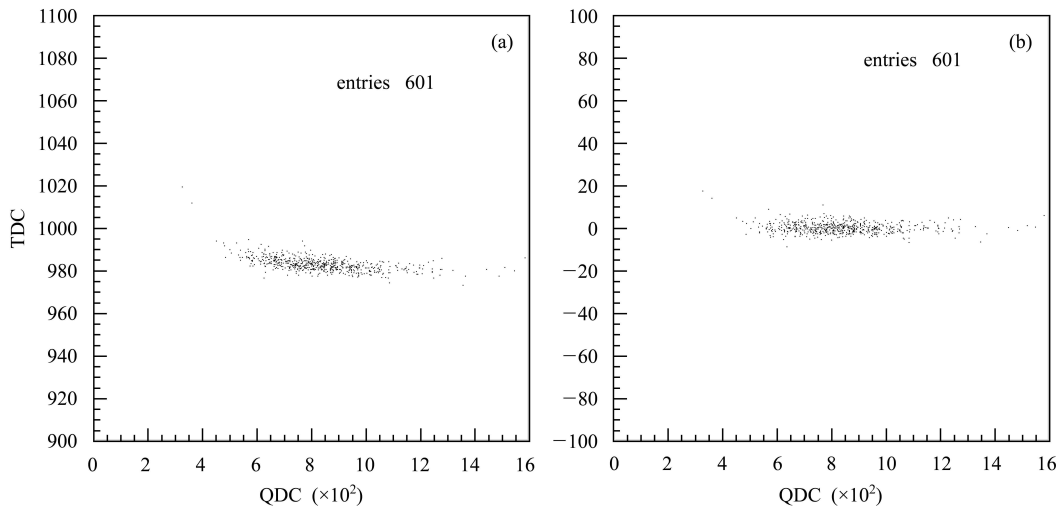


Fig. 7. (a) The original T-A correlation of MRPC; (b) the T-A correlation of MRPC after the T-A correction.

Since the leading-edge discriminators are used in the test, the timing dependence on the signal amplitude should be eliminated by the T-A correction. The time spectrum of  $T_0$  after the T-A correction is shown in Fig. 6. With the Gaussian fit function, the jitter of  $T_0$  is  $\sigma_{T_0} = 34$  ps.

The T-A correction is also applied to the MRPC signals. Fig. 7 shows the T-A correlation of MRPC before and after the correction, from which the effect of the correction can be clearly observed. A typical time spectrum of MRPC after the correction is shown in Fig. 8. After removing the contribution from the  $T_0$ , the resolution of MRPC is  $\sigma_{\text{MRPC}} = 45$  ps

Figure 9 shows the efficiency plateau of the MRPC. The detection efficiency is greater than 95%

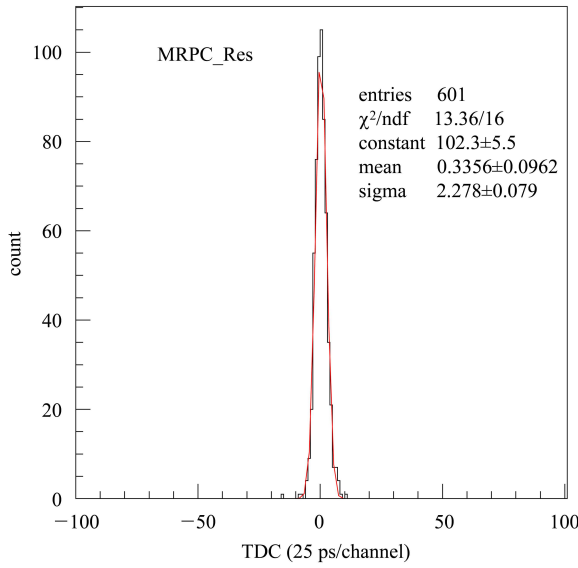


Fig. 8. The time spectrum of MRPC after T-A correction.

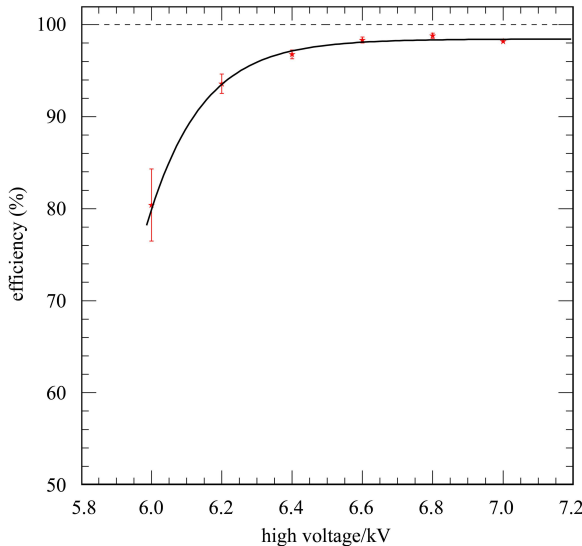


Fig. 9. The efficiency plateau.

when the applied HV is higher than  $\pm 6.6$  kV. The time resolution around the working HV is shown in Fig. 10 together with the corresponding detection efficiency. The working HV is chosen as  $\pm 6.8$  kV, where the detection efficiency is greater than 98% and the time resolution is the best.

In the beam test setup, the MRPC is fixed to a two-dimensional movable platform. If we define the incident direction of the beam as the  $z$  direction, the MRPC locates on the  $x$ - $y$  plane, as shown in Fig. 11. The performance of the MRPC is scanned in both directions.

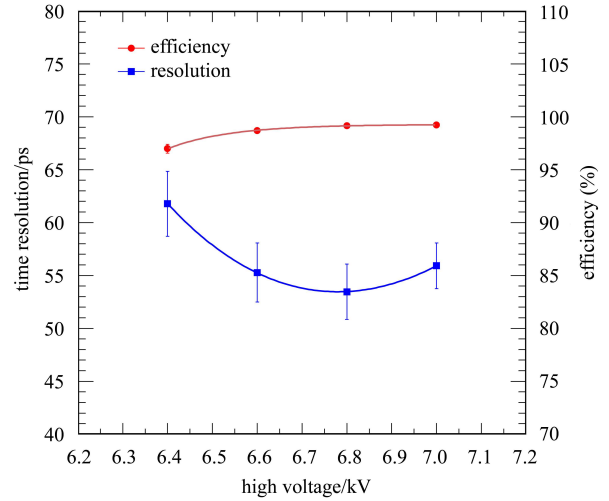


Fig. 10. Time resolution and detection efficiency vs. applied HV.

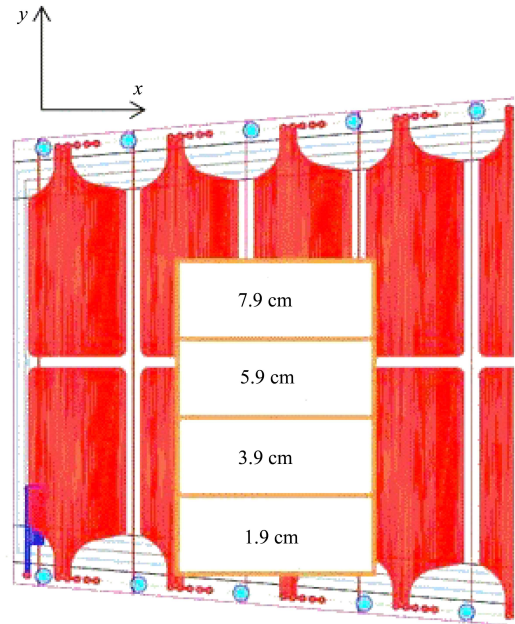


Fig. 11. The position scan along the  $y$  direction on the third shortest pad.

Figure 11 schematically shows the four positions scanned along the third shortest pad (in the  $y$  direction). The result is shown in Fig. 12. Notice that the width of the trigger is 2 cm and the length of this pad is 4.9 cm. At the position of  $y=1.9$  cm, it is clear from Fig. 11 that a part of the trigger is out of the pad. This is the reason why the time resolution is bad at this point. While at 5.9 cm, particles may

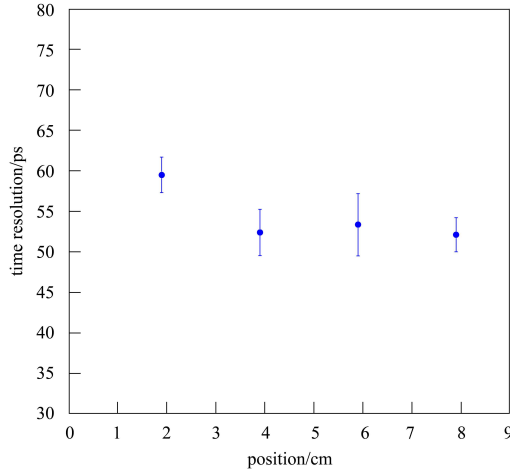


Fig. 12. The time resolution of the scan in the  $y$  direction.

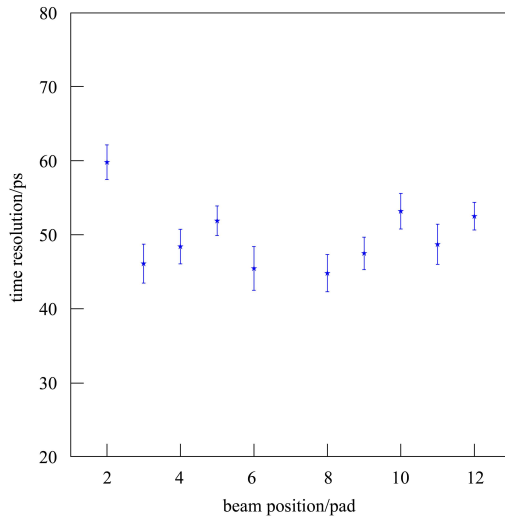


Fig. 13. The time resolution on different pads (scanned along the  $x$  direction, while  $y$  is fixed at 3.9 cm of Fig. 11.)

hit the edge of the pad or the gap between the upper and lower pads, causing the “sharing” of the induced charge between two pads. The time resolution at this position may become worse. When the trigger moves to 7.9 cm, the result is obtained from the upper pad since it is under the trigger.

The performances of the MRPC on different pads are also scanned since they are of different lengths. The result is shown in Fig. 13. The time resolution is around 50 ps on most of the pads and no dependence on pad length is found.

## 5 Summary

A prototype MRPC is designed for the upgrade of the BESIII ETOF. The prototype has  $2 \times 6 \times 0.22$  mm gas gaps and  $2 \times 12$  readout pads. The width of the pads is 2.5 cm, while the length ranges from 4.0 to 7.0 cm. The beam test executed in the BEPC E3 line indicates that the time resolution can reach 50 ps with a detection efficiency greater than 98%. There is no performance dependence on pad length. These results confirm the feasibility of upgrading the BESIII ETOF with MRPC technology.

The time resolution results discussed above include the incident position uncertainty along the pad direction. As shown in the beam test setup, the trigger size defined by the  $T_0$  system is 5 cm  $\times$  2 cm (Fig. 5), and the triggered width along the MRPC pad is 2 cm (Fig. 11). Since the signal propagation velocity along the pad is  $\sim 50$  ps/cm [9], the contribution from the position uncertainty is estimated to be around 30 ps. The contribution from the front end electronics (FEE) card (around 30 ps) is also included. Nevertheless, further tests are necessary with newly developed FEE cards (based on NINO chips) and the HPTDC DAQ system.

*We gratefully acknowledge Prof. Jiakai Li, Associate Prof. Zunjian Ke, Post-Dr. Guangpeng An and other members of the Beam Group of IHEP for their earnest support and help during the beam test.*

## References

- ZHAO Chuan, SUN Sheng-Sen et al. Chinese Physics C (HEP & NP), 2011, **35**(1): 72
- Williams M C S, Cerron E et al. Nucl. Instrum. Methods A, 1999, **434**(2-3): 362
- CHEN Hong-Fang, LI Cheng et al. High Energy Physics and Nuclear Physics, 2002, **26**(3): 201 (in Chinese)
- WU Jian, Bonner B et al. Nucl. Instrum. Methods A, 2005, **538**: 243
- ALICE Time of Flight Addendum. CERN/LHCC 2002-016, Addendum to ALICE TDR 8, 24 April 2002
- LI Cheng, CHEN Hong-Fang et al. High Energy Physics and Nuclear Physics, 2002, **26**(5): 455 (in Chinese)
- SHAO Ming, CHEN Hong-Fang et al. High Energy Physics and Nuclear Physics, 2004, **28**(7): 733 (in Chinese)
- LI Jia-Cai, WU Yuan-Ming et al. High Energy Physics and Nuclear Physics, 2004, **28**(12): 1269 (in Chinese)
- LI Liang, SHAO Ming et al. High Energy Physics and Nuclear Physics, 2007, **31**(6): 576 (in Chinese)